Journal of Microbiology (2017) Vol. 55, No. 11, pp. 862–870
DOI 10.1007/s12275-017-7104-1
eISSN 1976-3794
pISSN 1225-8873

# Magnetite production and transformation in the methanogenic consortia from coastal riverine sediments[§]

**Shiling Zheng[1†], Bingchen Wang[1,2†], Fanghua Liu[1*], and Oumei Wang[3*]**

[1]*Key Laboratory of Coastal Biology and Biological Resources Utilization, Yantai Institute of Coastal Zone Research, Chinese Academy of Sciences, Yantai 264003, P. R. China*
[2]*University of Chinese Academy of Sciences, Beijing 100049, P. R. China*
[3]*Binzhou Medical University, Yantai 264003, P. R. China*

(Received Aug 3, 2017 / Revised Sep 21, 2017 / Accepted Sep 22, 2017)

**Minerals that contain ferric iron, such as amorphous Fe(III) oxides (A), can inhibit methanogenesis by competitively accepting electrons. In contrast, ferric iron reduced products, such as magnetite (M), can function as electrical conductors to stimulate methanogenesis, however, the processes and effects of magnetite production and transformation in the methanogenic consortia are not yet known. Here we compare the effects on methanogenesis of amorphous Fe (III) oxides (A) and magnetite (M) with ethanol as the electron donor. RNA-based terminal restriction fragment length polymorphism with a clone library was used to analyse both bacterial and archaeal communities. Iron (III)-reducing bacteria including *Geobacteraceae* and methanogens such as *Methanosarcina* were enriched in iron oxide-supplemented enrichment cultures for two generations with ethanol as the electron donor. The enrichment cultures with A and non-Fe (N) dominated by the active bacteria belong to *Veillonellaceae*, and archaea belong to *Methanoregulaceae* and *Methanobacteriaceae*, *Methanosarcinaceae* (*Methanosarcina mazei*), respectively. While the enrichment cultures with M, dominated by the archaea belong to *Methanosarcinaceae* (*Methanosarcina barkeri*). The results also showed that methanogenesis was accelerated in the transferred cultures with ethanol as the electron donor during magnetite production from A reduction. Powder X-ray diffraction analysis indicated that magnetite was generated from microbial reduction of A and M was transformed into siderite and vivianite with ethanol as the electron donor. Our data showed the processes and effects of magnetite production and transformation in the methanogenic consortia, suggesting that significantly different effects of iron minerals on microbial methanogenesis in the iron-rich coastal riverine environment were present.**

***Keywords***: coastal riverine sediments, magnetite, ferrous iron, methane, iron (III)-reducing bacteria, methanogens

## Introduction

Fe (III) minerals as amorphous ferric oxides and crystalline iron oxides (*e.g.*, magnetite, goethite, hematite, and lepidocrocite) are ubiquitous in natural environments, can be reducible by iron (III)-reducing microorganisms to produce Fe (II) minerals (*e.g.*, magnetite, siderite, green rust, and vivianite) (Dong *et al.*, 2000; Hori *et al.*, 2015), having an important influence on the fate of a variety of environmental contaminants such as heavy metals, organic, and inorganic pollutants (Oren, 2014). Amorphous ferric oxides are readily reducible by iron (III)-reducing microorganisms, and have been reported to exhibit inhibitory effects on microbial methanogenesis in natural, and artificial environments. Competition for common electron donors (*e.g.*, hydrogen and acetate) between iron (III)-reducing microorganisms and methanogens can cause the inhibitory effect of iron oxides on methanogenesis (Bond and Lovley, 2002; Zhou *et al.*, 2014). Furthermore, the inhibition of methane production has demonstrated that it may result from the diversion of electron flow from methanogenesis to Fe (III) reduction (Bond and Lovley, 2002; Yamada *et al.*, 2014).

However, magnetite, as the most important biomineralisation product of iron (III) reduction is characterised as being the result of amorphous ferric oxide action by iron (III)-reducing microorganisms (Kostka and Nealson, 1995), which can act as electrical conductors to facilitate microbial methanogenesis in anoxic environments (Kato *et al.*, 2012b). During long-term incubation of ferrihydrite-supplemented paddy soil cultures, secondary minerals of magnetite from microbial ferrihydrite reduction accelerated methanogenesis instead of being suppressed in the initial microbial ferrihydrite reduction process (Zhuang *et al.*, 2015). Furthermore, microbial magnetite formation from ferrihydrite promoted direct interspecies electron transfer (DIET) between *Geobacter* and *Methanosarcina* co-cultures and thus facilitated methanogenesis (Tang *et al.*, 2016). In most of the methanogenic environments found, *Geobacter* species are abundant. Conductive minerals, such as magnetite or haematite, were also proposed to function as mediators between *Geobacter* and *Methanosarcina* species and facilitated methanogenesis in mineral-amended enrichment cultures with acetate or ethanol (Kato *et al.*, 2012a). Nanomagnetite-facilitating DIET has been reported in enrichment culture stimulating syntrophic butyrate oxidation and methane production, where *Geobacter* and *Methanosarcina* were the dominant genera, possibly us-

[†]These authors contributed equally to this work.
*For correspondence. (F. Liu) E-mail: fhliu@yic.ac.cn / (O. Wang) E-mail: omwang@aliyun.com
[§]Supplemental material for this article may be found at http://www.springerlink.com/content/120956.

ing nanomagnetite as an electron transfer mediator (Li *et al.*, 2015). Micron-sized magnetite amendments in methanogenic sludge promoted the conversion of propionate to methane which probably resulted from the establishment of a DIET, in which magnetite particles served as electron conduits between propionate-oxidising acetogens and carbon dioxide-reducing methanogens (Viggi *et al.*, 2014); however, in these studies, the reduction of magnetite had been considered as either undetectable, or quite small, in extent.

Magnetite is a mixed-valence iron oxide, in which $Fe^{2+}$ and $Fe^{3+}$ are close together in the edge-sharing chains of $FeO_6$ octahedra. It appeared that $Fe^{3+}$ is reduced to $Fe^{2+}$ from magnetite by dissimilatory Fe (III)-reducing bacteria (Kostka and Nealson, 1995). Recently, the reduction and transformation of magnetite was proposed as having occurred in anoxic methanogenic environments. In the presence of magnetite nanoparticles, significant amounts of $H_2$ and Fe (II) (vivianite) were formed with methane production in paddy soil enrichments suggesting that magnetite acted as an electron acceptor that could facilitate methane production from ethanol oxidation and the establishment of interspecies hydrogen transfer between iron (III)-reducing bacteria and methanogens (Yang *et al.*, 2015).

Iron oxides such as magnetite, amorphous Fe (III), oxides and Fe (II) minerals are abundant in soil and sediment environments, however, the environmental significance of different iron minerals on microbial methanogenesis in an iron-rich coastal riverine environment remains unexplored. The objective of our study was to investigate the processes and effects of magnetite production and transformation in the methanogenic consortia.

## Materials and Methods

### Enrichment cultivation

Sediment samples were collected from Jiehe River, Shandong Province, China. The characteristics of the sediment were evaluated by using standard methods as described previously (Zheng *et al.*, 2015): pH 5.84, organic C 0.525%, total nitrogen 0.112%, magnetic susceptibility $\chi_{LF}$ 142.28 (dry weight), total iron 14.89 mg/g (dry mass) and soil texture of the coarse sand fraction were measured.

Enrichment cultures were introduced by 10% (w/v) sediments into anaerobic fresh water enrichment (FWE) medium with 33 mmol/L acetate as the electron donor (Lovley and Phillips, 1986) for acquiring more iron (III)-reducing bacteria and methanogenic archaea. Then, each transfer was inoculated with 5% inocula into 40 ml medium in a 100 ml serum bottle under an atmosphere of $N_2/CO_2$ (80/20, V/V). After three transfers, enrichment cultures were transferred to the anaerobic DSMZ methanogenic medium 120 (DSM120) with 30 mmol/L ethanol as the electron donor (Rotaru *et al.*, 2014) for establishing syntrophic co-cultures as described briefly: 2.0 mmol/L $K_2HPO_4$, 1.7 mmol/L $KH_2PO_4$, 0.5 g/L $NH_4Cl$, 0.5 g/L $MgSO_4.7H_2O$, 1 g/L NaCl, 0.002 g/L $FeSO_4{\cdot}7H_2O$, 24 mmol/L $NaHCO_3$, 1 ml trace element solution SL-10, 0.2 g/L $CaCl_2{\cdot}H_2O$, 0.121 g/L Cysteine-HCl, 0.120 g/L $Na_2S{\cdot}9H_2O$, and 10 ml vitamin solution, the pH was adjusted to between 6.8 and 7.0. In the three enrichment cultures, two iron-oxide species were added to those enrichment mediums under the following conditions: amorphous Fe (III) oxides (A, 100 mmol/L), nano$Fe_3O_4$ (M, 5 mmol/L), and the control Non-Fe (N, without supplementing the specimen with extra iron oxides). Either amorphous Fe (III) oxides or nano-$Fe_3O_4$ was prepared as described previously (Lovley and Phillips, 1986; Kang *et al.*, 1996) and supplemented from stock solutions to give the desired final concentration before autoclaving. All cultures were incubated at 30°C in the dark under an atmosphere of $N_2/CO_2$ (80/20, V/V) without shaking.

### Chemical analysis

The gaseous samples (100 μl) were regularly collected from enrichment cultures using a pressure-lock analytical syringe. The concentrations of $CH_4$ and $H_2$ were evaluated using a gas chromatograph (GC) 7890A (Agilent Technologies) equipped with a flame ionisation detector (FID), and thermal conductivity detector (TCD), respectively.

Liquid samples were collected, centrifuged, and filtered through 0.22 μm filters as described (Li *et al.*, 2015). The concentrations of ethanol, acetate, and propionate in cultures were analysed using high-performance liquid chromatography (HPLC) 1260 Infinity (Agilent Technologies) with a Hi-plexH column equipped with a refractive index detector (RID).

The concentration of Fe (II) was extracted from enrichment cultures and each replicate of the assays was tested in triplicate as described previously (Achtnich *et al.*, 1995; Cummings *et al.*, 2000). Briefly, 0.5 ml of the enrichment cultures was mixed with 4.5 ml 0.5 mol/L HCl, after incubation, and the resulting acidified sub-sample was reacted with 0.1% ferrozine reagent, and quantified at 562 nm by UV-Vis spectrophotometer.

### Molecular analyses

When the methane production level reached its plateau in each enrichment culture, microbial RNA extracts were assayed by using a bead-beating protocol (Shrestha *et al.*, 2009). Briefly, cell lysis was homogenised using a FastPrep-24 instrument (MP Biomedicals). Total nucleic acids were treated with gDNA Eraser (TaKaRa) to remove co-extracted DNA. RNA was conformed to be DNA-free by the absence of PCR products by amplifying 16S rRNA genes with universal primers Ba27f/Ba907r for bacteria, and Ar109f/Ar915r for archaea (Zheng *et al.*, 2015).

Reverse transcription was performed on the resulting cDNA products according to the instructions governing the use of the PrimeScript™ RT reagent Kit (TaKaRa) after RNA denaturation at 70°C for 10 min, followed by an incubation step at 37°C for 50 min.

Terminal restriction fragment length polymorphism (T-RFLP) was performed as described previously (Liu and Conrad, 2010; Bokulich *et al.*, 2012). Bacterial and archaeal 16S rRNA genes were amplified from community cDNA with the primers labelled with 6-carboxyfluorescein (FAM)-Ba27f/Ba907r and Ar109f/Ar915r-FAM. Amplification was performed as follows: 2 min at 94°C, followed by 30 cycles consisting of denaturation for 30 sec at 94°C, annealing for 30 sec at 55°C, extension for 1 min at 72°C, and a final exten-

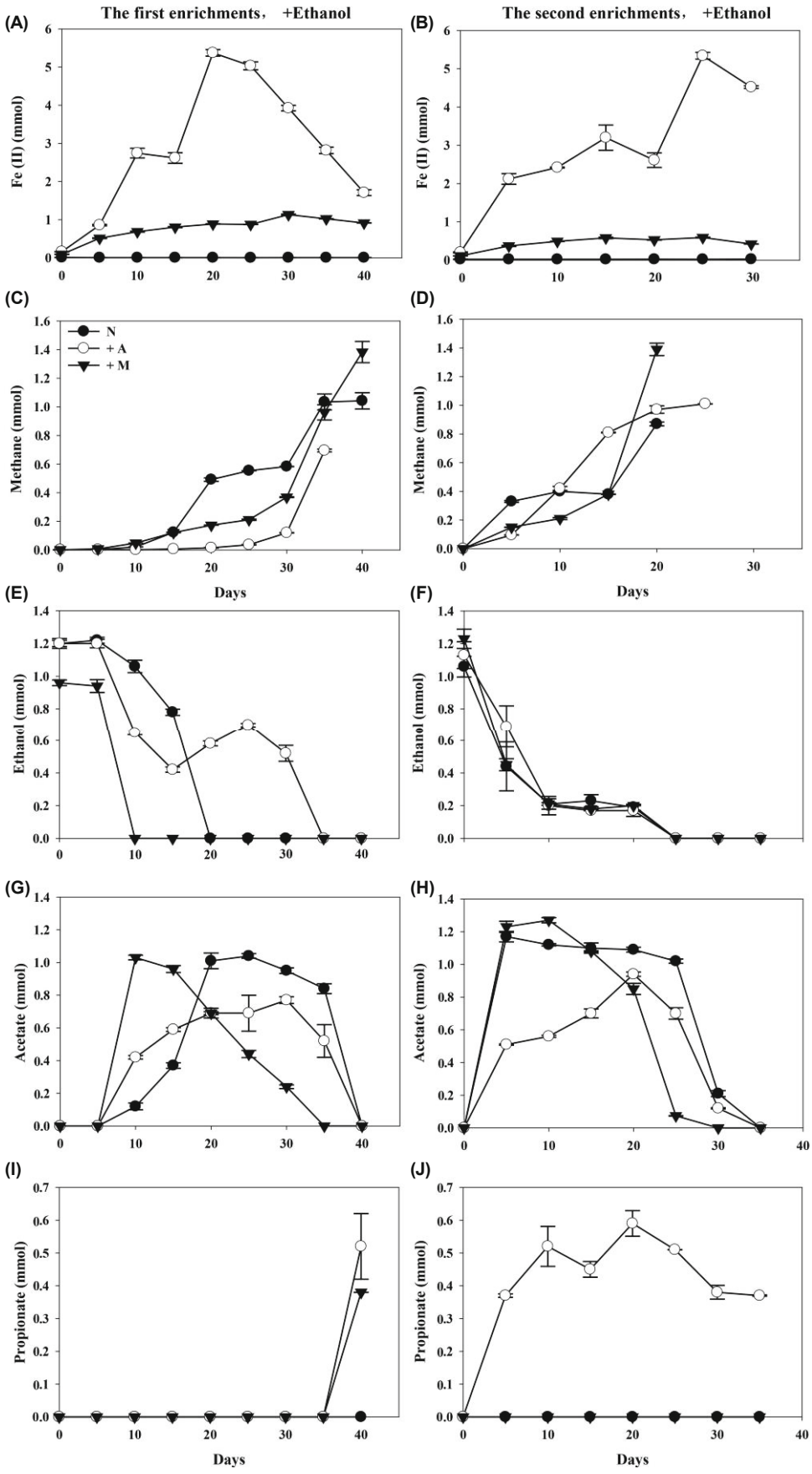


**Fig. 1. Ferrous iron and methane production, ethanol consumption, acetate production and consumption, and propionate production in enrichment cultures.** Time-courses of ferrous iron production (A, B) methane production (C, D), ethanol consumption (E, F), acetate production and consumption (G, H), and propionate production (I, J) in the first and second DSM120 enrichment cultures with ethanol as a substrate in the absence, or presence, of 100 mmol/L amorphous Fe(III) oxides and 5 mmol/L nano$Fe_3O_4$ without supplementing with extra iron oxides as in the control non-Fe (N). Data are presented in triplicate and standard deviations are shown for each data point: data were tested for significant differences ($P < 0.05$) by one-way ANOVA.

sion at 72°C for 10 min. PCR products were purified and digested using *Msp*I for bacteria and *Taq*I for archaea respectively, and subsequently analysed using an automated sequencer ABI PRISM 3730XL (Applied Biosystems). The relative abundance of T-RFs was estimated and expressed as the percentage distribution of the different T-RF peak heights within each bacterial and archaeal community fingerprint.

Bacterial and archaeal clone libraries of 16S rRNA genes were constructed from cDNA samples. PCR was performed with the primers without FAM labelling. Amplicons were cloned into *Escherichia coli* DH5α and sequenced at Life Technologies. Nucleotide sequences were analysed with DNA-Star 7.0 (Madison). All positive sequences were subjected to simulated digestion using DNAMAN 8.0 (Lynnon Biosoft) software and checked against actual T-RFs patterns in the T-RFLP maps.

Phylogenetic analysis of the sequences from bacterial and archaeal clone libraries was performed using the MEGA 7.0 (Kumar *et al.*, 2016) software package with a neighbour-joining method. Sequence data obtained from clone libraries and isolates in this study have been submitted to the GenBank database under accession numbers: KT008240-KT008243, KT008226-KT008230, KT008235-KT008237, KX061923-KX061927, and KU933361-KU933363 for bacteria, and KT008244-KT008245, KT008247-KT008250, KT008252, KT008261, and KX061918-KX061922 for methanogenic archaea.

### X-ray diffraction (XRD) analysis

All cultures were collected at the end of enrichment cultivation under anaerobic conditions and washed several times before natural drying, and were characterised by powder X-ray diffraction using a diffractometer (D/MAX-2000, Rigaku) with monochromatic CuKα radiation ($\lambda$ = 0.15406 nm) at a scan rate of 0.02 2$\theta$/sec. Data analyses were performed using PANalytical Highscore Plus Version 3.0 software.

## Results

### Effect of iron oxides on methanogenesis from ethanol metabolism

In all anaerobic incubation experiments, syntrophic enrichment cultures were established to investigate how iron oxides affected methanogenesis. First, microbial communities were enriched by three transfers of coastal gold mining riverine sediments with, or without, iron oxide treatments when acetate was used as the electron donor (Supplementary data Fig. S1). Second, the enrichment cultures were transferred with ethanol as alternative electron donor for two generations. Soluble ferrous irons in enrichment cultures were produced from the first to the second generation, and approximately 5.34 ± 0.087 mmol, and 0.59 ± 0.011 mmol ferrous iron were accumulated in the second generation of A and M-supplemented cultures, respectively (Fig. 1B); however, ferrous iron was not detected in the control group of N cultures on the same substrate (Fig. 1A and B).

Under ethanol-amended conditions, the lag phase of methane production was shortened from the first to the second generation. Compared with N cultures, methane production was accelerated in the A-supplemented cultures of the second generation while it was largely suppressed in the first generation, in which the maximum amount of methane increased from 0.70 ± 0.01 at 35 days to 1.01 ± 0.00077 mmol at 25 days. Similarly, methane production was suppressed in the presence of supplemented M during the first generation at 35 days compared with N cultures, whereas it rapidly reached 1.38 ± 0.074 mmol at 40 days. Methane production was also accelerated in the second generation: the amount of methane increased to 1.39 ± 0.043 mmol at 20 days. On the contrary, the amount of methane production decreased from the first to the second generation (1.04 ± 0.057 mmol vs 0.87 ± 0.013 mmol; $n$ = 3) in N cultures. During the incubation period, no hydrogen was detected in these enrichment cultures.

Acetate and propionate were the soluble intermediates detected during ethanol degradation to methane in the presence of iron oxides (Fig. 1E–J). In M-supplemented cultures, the accumulation of acetate reached a peak in a shorter period (the first generation *versus* the second generation, 10 days vs 5 days; indicative of faster ethanol oxidation) and was depleted faster (35 days vs 30 days; indicative of faster methane production) (Fig. 2G and H). Interestingly, around 0.52 ± 0.1 mmol propionate was produced in A-supplemented cultures at 40 days in the first generation and this continued until the second generation. While in M-supplemented cultures, propionate transiently accumulated at 40 days in the first generation and was further consumed in enrichments of the second generation (Fig. 2I and J).

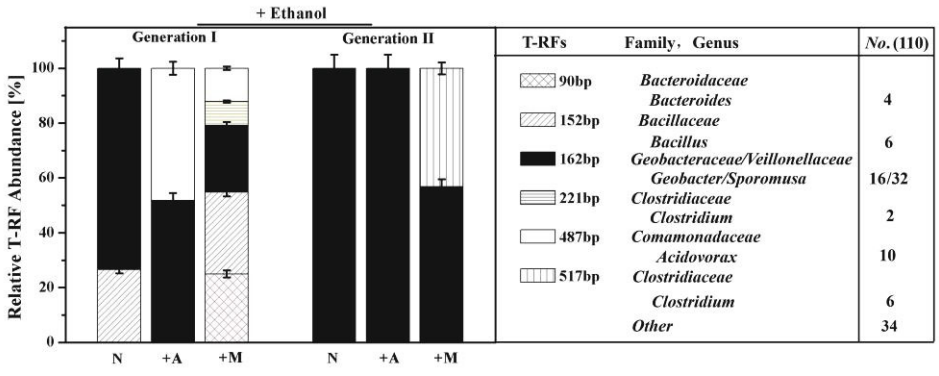


**Fig. 2. Community characteristics of bacterial communities after the enrichment of incubations with ethanol as the substrate, as revealed by T-RFLP and clone libraries of the 16S rRNA gene.** Relative abundance of different bacterial T-RFs from RNA extracted from enrichment cultures (with, or without, amorphous Fe (III) oxides and nano$Fe_3O_4$ treatment as N, A, and M). T-RF fingerprints were generated using the *Msp* I restriction enzyme. The relative T-RF abundance of rRNA was presented from triplicate RNA extractions for each sample.

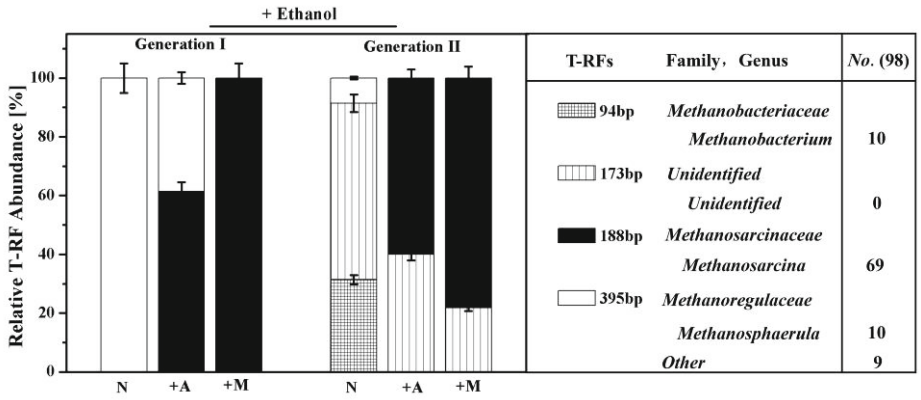


**Fig. 3. Community characteristics of archaeal communities after the enrichment of incubations with ethanol as the substrate, as revealed by T-RFLP and clone libraries of the 16S rRNA genes.** Relative abundance of different bacterial T-RFs from RNA extracted from enrichment cultures [with, or without, amorphous Fe (III) oxides and nano-$Fe_3O_4$ treatment as N, A, and M]. T-RF fingerprints were generated using the *Taq*I restriction enzyme. The relative T-RF abundance of rRNA was presented from triplicate RNA extractions for each sample.

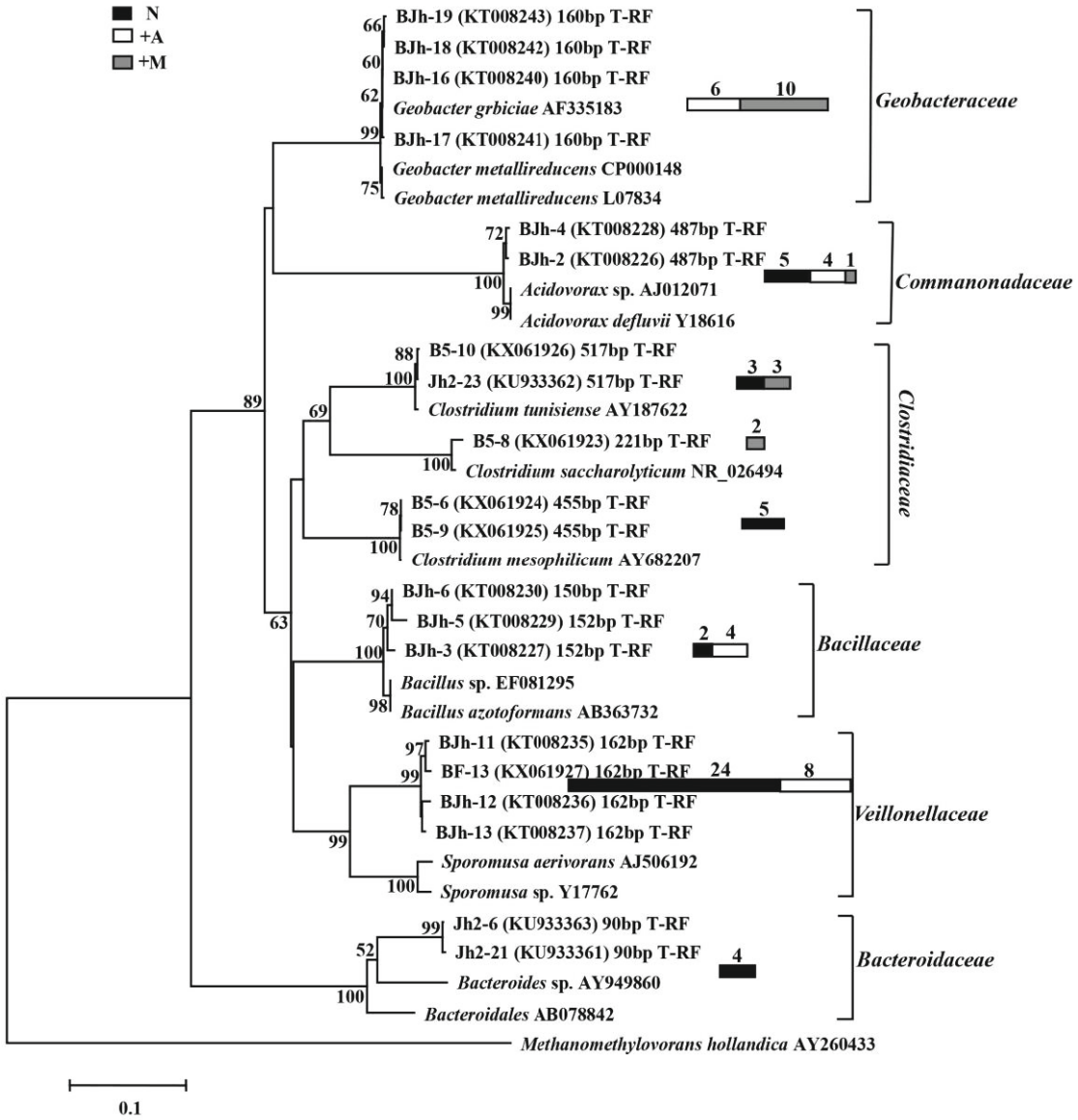


**Fig. 4. Neighbour-joining phylogenetic tree of representative bacterial 16S rRNA gene clones generated from RNA extracted from enrichment cultures.** Numbers of T-RF lengths are shown in base pair terms. An association with the sequence of the highest similarity in the database and GenBank accession numbers of representative sequences (in brackets) and reference sequences are as indicated. The numbers of clones in the clone libraries are indicated. The scale bars represent 10% sequence divergence. *Methanomethylovoranshollandica* was selected as the out-group of the bacterial phylogenetic tree.

According to a theoretical stoichiometric equation for methanogenesis from ethanol oxidation ($2CH_3CH_2OH \rightarrow 3CH_4 + CO_2$) (Kato *et al.*, 2012a; Rotaru *et al.*, 2014) in the second generation, the calculation suggested that 59.3% and 75.6% of the electrons from ethanol oxidation were respectively recovered in methane in the cultures with A and M amendment, while in N cultures, 54.7% of the electrons from ethanol oxidation were recovered in methane.

### Iron (III)-reducing bacteria and methanogens occurring in the methanogenic consortia

In syntrophic ethanol oxidation enrichment cultures, the activities of iron (III)-reducing bacteria and methanogens were seen in the iron oxide-supplemented enrichment cultures. After a certain incubation period, the relative abundance of the bacterial terminal restriction fragments (T-RF) was as shown in Fig. 2. For rRNA, with ethanol as the electron donor in the presence or absence of iron oxides, the bacterial communities dynamically varied from the first to the second generation, in which 160–162 bp T-RF was exclusively predominant in all enrichment cultures. Except for the 160–162 bp T-RF, 487 bp T-RF dominated in A-supplemented cultures of the first generation, 90 bp, 152 bp, 221 bp, 487 bp, and 517 bp T-RFs dominated in A-supplemented cultures, while 152 bp T-RF dominated in N cultures.

Similarly, the relative abundance of the archaeal T-RF at the same samples was also analysed (Fig. 3). For rRNA with ethanol as the electron donor, 188 bp and/or 395 bp T-RFs were predominant in enrichments of the first generation, and 94 bp, 173 bp, 188 bp, and 395 bp T-RFs were predominant in the second enrichment cultures.

To affiliate the detected T-RFs to phylogenetic bacterial and archaeal groups, six clone libraries (three bacterial clone libraries and three archaeal clone libraries) were generated using all three samples. Sequence data were analysed to assign, albeit tentatively, major T-RFs, which were observed in different bacterial and archaeal fingerprints to defined phylogenetic lineages. Thus, the predominance of 90 bp, 152 bp, 160–162 bp, and 487 bp T-RFs represented members of *Bacteroidaceae*, *Bacillaceae*, *Geobacteraceae*/*Veillonellaceae*, and *Comamonadaceae*, respectively. 221 bp and 517 bp T-RFs all represented members of *Clostridiaceae*. Similarly, the predominant 188 bp T-RF represented members of *Methanosarcinaceae*, which were dominant in the rRNA clone libraries with the supplementation of iron oxides. 94 bp and 395 bp T-RFs represented members of *Methanobacteriaceae* and *Methanoregulaceae*, respectively, which mainly dominated the rRNA clone libraries of N cultures. However 173 bp, dominant in the three enrichment cultures, was not detected for a corresponding clone. This result should be further investigated. The phylogenetic trees of selected representative bacterial and archaeal clones, and their closest representative species, were constructed (Figs. 4 and 5). The phylogenic types detected showed that the bacterial 160 bp T-RF represented members of *Geobacteraceae* in A and M-supplemented cultures, while the 162 bp T-RF represented members of *Veillonellaceae* dominant in N and A cultures with ethanol as the

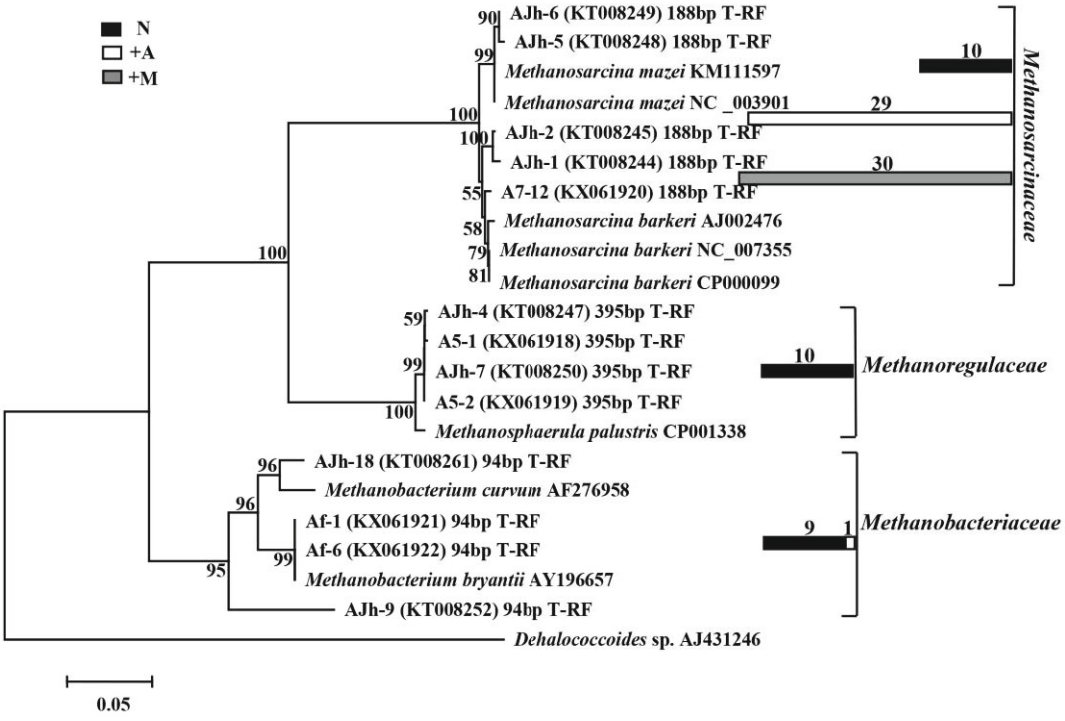


**Fig. 5. Neighbour-joining phylogenetic tree of representative archaeal 16S rRNA gene clones generated from RNA extracted from enrichment cultures.** Numbers of T-RF lengths are shown in base pair terms. An association with the sequence of the highest similarity in the database and GenBank accession numbers of representative sequences (in brackets) and reference sequences are as indicated. The numbers of clones in the clone libraries are indicated. The scale bars represent 5% sequence divergence. *Dehalococcoides* sp. was selected as the out-group of the archaeal phylogenetic tree.

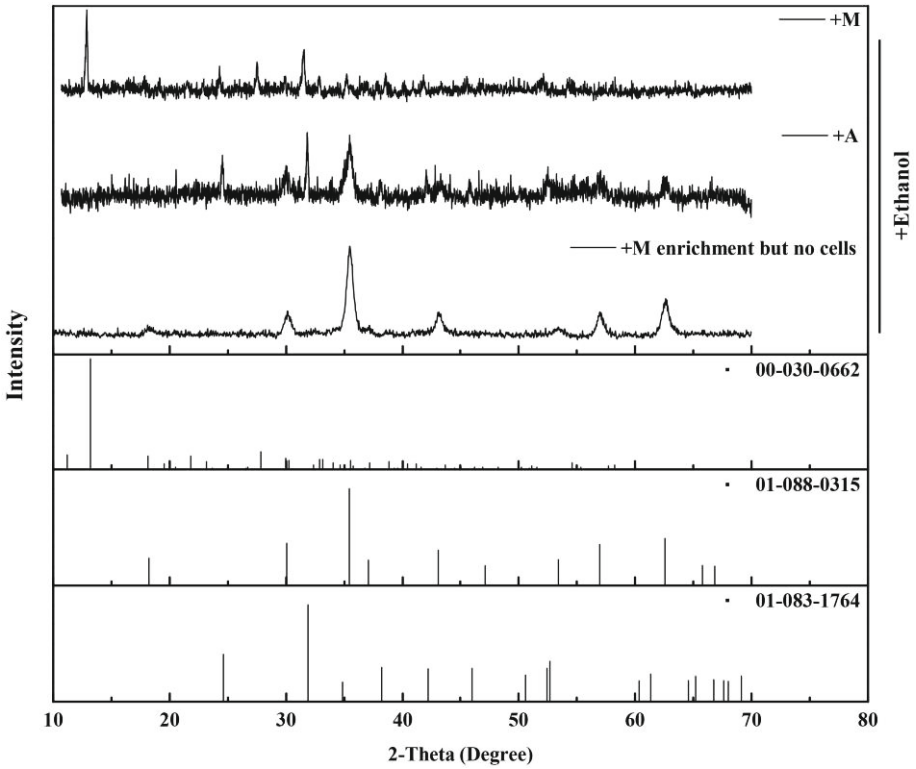


**Fig. 6. The X ray diffraction spectrum of amendments of amorphous Fe (III) (A) oxides and nano-$Fe_3O_4$ (M) after incubation with ethanol as the substrate.** Nano-$Fe_3O_4$ enrichment (but with no cells) comprises the control group here. 01-088-0315 is the standard card for $Fe_3O_4$, 01-083-1764 is the standard card for $FeCO_3$, and 00-030-0662 is the standard card for $Fe_3(PO4)_2{\cdot}8H_2O$.

electron donor. Sequences of the 188 bp T-RF were closely related to methanogen *Methanosarcina barkeri* that dominated the M-supplemented cultures, whereas other sequences of 188 bp T-RF were most closely related to *Methanosarcina mazei* (dominant in A-supplemented, and N, cultures).

### Mineral transformation of iron oxides associated with microbial reduction after incubation

At the end of the incubation experiments, iron oxide-supplemented precipitates were subjected to powder X-ray diffraction (XRD) analysis (Fig. 6). The mineral production and transformation from microbial reduction of A and M cultures were analysed with ethanol as the electron donor. During microbial ferric oxides reduction, A was transformed into magnetite ($Fe_3O_4$) and siderite ($FeCO_3$), which were the dominant mineralisation products accounting for 81.52% and 18.48% of the total ferrous iron obtained by microbial reduction, M was transformed into siderite ($FeCO_3$) and vivianite [$Fe_3(PO_4)_2{\cdot}8H_2O$], which accounted for approximately 53.75% and 46.25% of the total ferrous iron present based on the concentration of bicarbonate and phosphate in the medium, respectively. This indicated that biogenic magnetite could be produced from A, and that siderite and vivianite could be transformed from M by iron (III)-reducing microorganisms with ethanol as the electron donor.

## Discussion

The study demonstrated the processes and effects of magnetite production and transformation in the methanogenic consortia and compared the effects on methanogenesis of amorphous Fe (III) oxides (A) and magnetite (M) with ethanol as the electron donor. The results have implications for our understanding of the mechanisms by which mineral transformations affect microbial methanogenesis in natural environments.

In the presence of A, direct inhibition of methanogenesis has been observed under ethanol-amended conditions during the first generation, while methanogenesis was accelerated in the second generation compared with the control N enrichments. A similar result was documented in a previous study wherein methanogenesis was not suppressed, but was enhanced as a result of the long-term effects of ferrihydrite supplementation (Zhuang *et al.*, 2015). M-supplemented cultures produced accelerated methanogenesis except in the earlier stage of the first generation under ethanol-amended conditions. This result was different from that previously reported, where the amendment of magnetite as conductive iron-oxide mineral stimulated methanogenesis from the first to the second enrichment of rice paddy soil with acetate or ethanol as the substrate (Kato *et al.*, 2012a). This discrepancy perhaps derived from the geochemical characteristics of the unique coastal riverine ecosystem as the microbial inoculation medium. Another reason was hypothesised as being related to mineral transformation processes involving microbial reduction that affected the methanogenesis.

Magnetite is an important mineral product of microbial Fe (III) reduction and this process depends on geochemical parameters in various natural environments (Piepenbrock *et al.*, 2011). During microbial incubation, we have found $Fe^{3+}$ of A and M were firstly reduced to $Fe^{2+}$ by iron (III)-reducing microorganisms leading to the formation of the secon-

dary mineral products, which further affected methanogenic activities. Magnetite could be easily produced from A-supplemented cultures, and then biogenic magnetite (with ethanol as the electron donor), as an electrical conductor, facilitated methanogenesis. While M in cultures was observed to suffer a loss of electrical conductivity and was transformed into siderite and vivianite, the formation of siderite and vivianite has been widely observed in the microbial reduction of Fe (III)-containing minerals, when carbonate (bicarbonate) and phosphate concentrations are sufficiently high. This could be correlated with the observation of a small amount of siderite formation arising as a result of biogenic magnetite reduction in A-supplemented cultures. Considering these results, it is therefore likely that the active microbial communities could be involved in the process of magnetite production and transformation.

Next, we analysed the majority of microbial communities that were involved in mineral transformation. The results from the analysis of T-RFLP and clone libraries showed that some phylogenetic groups occurred specifically and did not depend on the amendment of iron-oxide species, for instance, *Geobacter* species, which are closely related to *Geobacter grbiciae* and *Geobacter metallireducens* of *Deltaproteobacteria* shared large fractions as active members of dissimilatory iron-reducing bacteria (DIRB) that dominated in both iron oxide-amended enrichments. It was deduced that these different *Geobacter* species may play a key role in the process of ferric iron reduction; however, the predominance of 162 bp T-RF in N and A-supplemented cultures, which has a similar T-RF to *Geobacter* species, represented members of *Veillonellaceae*. Some species of this family are considered to be iron reducing and homoacetogenic bacteria (Boga *et al.*, 2003; Peng *et al.*, 2016) that are perhaps involved in ferric iron reduction in the A-supplemented cultures.

Previous studies have showed that magnetite accelerates methane production in methanogenic environments, in which it is accompanied by the enrichment of *Geobacter* and *Methanosarcina* species. The enhanced methane production can be attributed to enhanced electron transfer through magnetite to methanogens. Being concerned with their action as methanogens in this study, *Methanobacterium* spp. are characterised as hydrogenotrophic methanogens, their growth is restricted from $H_2/CO_2$ and/or formate (Schirmack *et al.*, 2014; Kern *et al.*, 2015). These species were mainly detected in the N cultures with ethanol as the substrate, and we deduced that hydrogenotrophic methanogenesis perhaps occurred in these cultures on account of its energy metabolism. In addition, *Methanosphaerula* spp., a hydrogenotrophic methanogen, uses formate as its only methanogenic substrate (Cadillo-Quiroz *et al.*, 2009), which was also exclusively predominant in N enrichments. This result suggested that *Geobacter* species could not establish a syntrophic association with hydrogenotrophic methanogens in N enrichments because co-cultures initiated with *Geobacter* sp. that could not utilise hydrogen and formate were also present. *Methanosarcina* spp. are known for utilising broad spectrum substrates for methanogenesis, including $H_2/CO_2$, acetate, and various methyl compounds (Gonnerman *et al.*, 2013; Jablonski *et al.*, 2015). In addition, *Methanosarcina* spp. are also candidates for roles as the syntrophic partners of *Geobacter* spp. in some environments or laboratory co-cultures (Kato *et al.*, 2012a; Rotaru *et al.*, 2014). This study showed that *Methanosarcina* species mainly grew in both iron oxide-supplemented cultures, but the identified species in clone libraries were different. *Methanosarcina mazei* has been reported to be capable of reducing structural Fe (III) alone in illite-smectite minerals (Zhang *et al.*, 2012), which was preferred in A-supplemented cultures in this study. While *Methanosarcina barkeri* was abundantly dominant in magnetite-supplemented cultures which suggested that *Methanosarcina barkeri* perhaps created a syntrophic association with *Geobacter* spp. and performed IET in the presence of magnetite.

Therefore, further research is underway in our laboratory to confirm the possible IET between *Methanosarcina mazei*, *Methanosphaerula* spp. (*Methanosphaerula palustris*), or *Methanobacterium* spp. which created syntrophic associations with *Geobaceter* species in the presence, or absence, of iron oxides.

## Acknowledgements

We thank Yunshen You (Peking University) for performing X-ray diffraction analysis of the mineral specimens in this study. This research was supported by the General Programme (Nos. 41371257 and 41573071) and the Major Research plan (No. 91751112) of the National Natural Science Foundation of China, the Key Research Project of Frontier Science (No. QYZDJ-SSW-DQC015), the Natural Science Foundation of Shandong Province (Grant no. ZR2016DQ12), and the Young Taishan Scholars Programme (No. tsqn 20161054).

## Conflict of Interests

The authors declare there are no competing interests.

## References

**Achtnich, C., Bak, F., and Conrad, R.** 1995. Competition for electron donors among nitrate reducers, ferric iron reducers, sulfate reducers, and methanogens in anoxic paddy soil. *Biol. Fertil. Soils* **19**, 65–72.

**Boga, H.I., Ludwig, W., and Brune, A.** 2003. *Sporomusa aerivorans* sp. nov., an oxygen-reducing homoacetogenic bacterium from the gut of a soil-feeding termite. *Int. J. Syst. Evol. Microbiol.* **53**, 1397–1404.

**Bokulich, N.A., Bamforth, C.W., and Mills, D.A.** 2012. A review of molecular methods for microbial community profiling of beer and wine. *J. Am. Soc. Brew. Chem.* **70**, 150–162.

**Bond, D.R. and Lovley, D.R.** 2002. Reduction of Fe(III) oxide by methanogens in the presence and absence of extracellular quinones. *Environ. Microbiol.* **4**, 115–124.

**Cadillo-Quiroz, H., Yavitt, J.B., and Zinder, S.H.** 2009. *Methanosphaerula palustris* gen. nov., sp. nov., a hydrogenotrophic methanogen isolated from a minerotrophic fen peatland. *Int. J. Syst. Evol. Microbiol.* **59**, 928–935.

**Cummings, D.E., March, A.W., Bostick, B., Spring, S., Caccavo, F., Fendorf, S., and Rosenzweig, R.F.** 2000. Evidence for microbial Fe (III) reduction in anoxic, mining-impacted lake sediments (Lake Coeur d'Alene, Idaho). *Appl. Environ. Microbiol.*

**66**, 154–162.

**Dong, H.L., Fredrickson, J.K., Kennedy, D.W., Zachara, J.M., Kukkadapu, R.K., and Onstott, T.C.** 2000. Mineral transformation associated with the microbial reduction of magnetite. *Chem. Geol.* **169**, 299–318.

**Gonnerman, M.C., Benedict, M.N., Feist, A.M., Metcalf, W.W., and Price, N.D.** 2013. Genomically and biochemically accurate metabolic reconstruction of *Methanosarcina barkeri* Fusaro, iMG746. *Biotech. J.* **8**, 1070–1129.

**Hori, T., Aoyagi, T., Itoh, H., Narihiro, T., Oikawa, A., Suzuki, K., Ogata, A., Friedrich, M.W., Conrad, R., and Kamagata, Y.** 2015. Isolation of microorganisms involved in reduction of crystalline iron (III) oxides in natural environments. *Front. Microbiol.* **6**, 386.

**Jablonski, S., Rodowicz, P., and Lukaszewicz, M.** 2015. Methanogenic archaea database containing physiological and biochemical characteristics. *Int. J. Syst. Evol. Microbiol.* **65**, 1360–1368.

**Kang, Y.S., Risbud, S., Rabolt, J.F., and Stroeve, P.** 1996. Synthesis and characterization of nanometer-size $Fe_3O_4$ and $\gamma$-$Fe_2O_3$ particles. *Chem. Mater.* **8**, 2209–2211.

**Kato, S., Hashimoto, K., and Watanabe, K.** 2012a. Methanogenesis facilitated by electric syntrophy via (semi) conductive iron-oxide minerals. *Environ. Microbiol.* **14**, 1646–1654.

**Kato, S., Hashimoto, K., and Watanabe, K.** 2012b. Microbial interspecies electron transfer via electric currents through conductive minerals. *Proc. Natl. Acad. Sci. USA* **109**, 10042–10046.

**Kern, T., Linge, M., and Rother, M.** 2015. *Methanobacterium aggregans* sp. nov., a hydrogenotrophic methanogenic archaeon isolated from an anaerobic digester. *Int. J. Syst. Evol. Microbiol.* **65**, 1975–1980.

**Kostka, J.E. and Nealson, K.H.** 1995. Dissolution and reduction of magnetite by bacteria. *Environ. Sci. Technol.* **29**, 2535–2540.

**Kumar, S., Stecher, G., and Tamura, K.** 2016. MEGA7: Molecular evolutionary genetics analysis version 7.0 for bigger datasets. *Mol. Biol. Evol.* **33**, 1870–1874.

**Li, H., Chang, J., Liu, P., Fu, L., Ding, D., and Lu, Y.** 2015. Direct interspecies electron transfer accelerates syntrophic oxidation of butyrate in paddy soil enrichments. *Environ. Microbiol.* **17**, 1533–1547.

**Liu, F. and Conrad, R.** 2010. *Thermoanaerobacteriaceae* oxidize acetate in methanogenic rice field soil at 50 degrees C. *Environ. Microbiol.* **12**, 2341–2354.

**Lovley, D.R. and Phillips, E.J.P.** 1986. Organic-matter mineralization with reduction of ferric iron in anaerobic sediments. *Appl. Environ. Microbiol.* **51**, 683–689.

**Oren, A.** 2014. The family *Methanosarcinaceae*, pp. 259–281. *In* Rosenberg, E., De Long, E.F., Lory, S., Stackebrandt, E., and Thomson, F. The Prokaryotes. Springer Berlin, Heidelberg, Germany.

**Peng, Q.A., Shaaban, M., Wu, Y., Hu, R., Wang, B., and Wang, J.** 2016. The diversity of iron reducing bacteria communities in subtropical paddy soils of China. *Appl. Soil Ecol.* **101**, 20–27.

**Piepenbrock, A., Dippon, U., Porsch, K., Appel, E., and Kappler, A.** 2011. Dependence of microbial magnetite formation on humic substance and ferrihydrite concentrations. *Geochim. Cosmochim. Acta* **75**, 6844–6858.

**Rotaru, A.E., Shrestha, P.M., Liu, F., Markovaite, B., Chen, S., Nevin, K., and Lovley, D.** 2014. Direct interspecies electron transfer between *Geobacter metallireducens* and *Methanosarcina barkeri*. *Appl. Environ. Microbiol.* **80**, 4599–4605.

**Schirmack, J., Mangelsdorf, K., Ganzert, L., Sand, W., Hillebrand-Voiculescu, A., and Wagner, D.** 2014. *Methanobacterium movilense* sp. nov., a hydrogenotrophic, secondary-alcohol-utilizing methanogen from the anoxic sediment of a subsurface lake. *Int. J. Syst. Evol. Microbiol.* **64**, 522–527.

**Shrestha, P.M., Kube, M., Reinhardt, R., and Liesack, W.** 2009. Transcriptional activity of paddy soil bacterial communities. *Environ. Microbiol.* **11**, 960–970.

**Tang, J., Zhuang, L., Ma, J., Tang, Z., Yu, Z., and Zhou, S.** 2016. Secondary mineralization of ferrihydrite affects microbial methanogenesis in *Geobacter-Methanosarcina* cocultures. *Appl. Environ. Microbiol.* **82**, 5869–5877.

**Viggi, C.C., Rossetti, S., Fazi, S., Paiano, P., Majone, M., and Aulenta, F.** 2014. Magnetite particles triggering a faster and more robust syntrophic pathway of methanogenic propionate degradation. *Environ. Sci. Technol.* **48**, 7536–7543.

**Yamada, C., Kato, S., Ueno, Y., Ishii, M., and Igarashi, Y.** 2014. Inhibitory effects of ferrihydrite on a thermophilic methanogenic community. *Microbes Environ.* **29**, 227–230.

**Yang, Z.M., Shi, X.S., Wang, C.S., Wang, L., and Guo, R.B.** 2015. Magnetite nanoparticles facilitate methane production from ethanol via acting as electron acceptors. *Sci. Rep.* **5**, 16118.

**Zhang, J., Dong, H.L., Liu, D., Fischer, T.B., Wang, S., and Huang, L.Q.** 2012. Microbial reduction of Fe(III) in illite-smectite minerals by methanogen *Methanosarcina mazei*. *Chem. Geol.* **292**, 35–44.

**Zheng, S., Zhang, H., Li, Y., Zhang, H., Wang, O., Zhang, J., and Liu, F.** 2015. Co-occurrence of *Methanosarcina mazei* and *Geobacteraceae* in an iron (III)-reducing enrichment culture. *Front. Microbiol.* **6**, 941.

**Zhou, S., Xu, J., Yang, G., and Zhuang, L.** 2014. Methanogenesis affected by the co-occurrence of iron (III) oxides and humic substances. *FEMS Microbiol. Ecol.* **88**, 107–120.

**Zhuang, L., Xu, J.L., Tang, J., and Zhou, S.G.** 2015. Effect of ferrihydrite biomineralization on methanogenesis in an anaerobic incubation from paddy soil. *J. Geophys. Res. Biogeosci.* **120**, 876–886.